

Structural control of cable-stayed bridges under traveling earthquake wave excitation

Shehata E Abdel Raheem^{*1, 2}

¹Department of Civil Engineering, College of Engineering, Taibah University,
Madinah 41411, Saudi Arabia

²Department of Civil Engineering, Faculty of Engineering, Assiut University, Assiut 71516, Egypt

(Received July 26, 2017, Revised October 30, 2017, Accepted October 31, 2017)

Abstract. Post-earthquake damages investigation in past and recent earthquakes has illustrated that the ground motion spatial variation plays an important role in the structural response of long span bridges. For the structural control of seismic-induced vibrations of cable-stayed bridges, it is extremely important to include the effects of the ground motion spatial variation in the analysis for design of an effective control system. The feasibility and efficiency of different vibration control strategies for the cable-stayed bridge under multiple support excitations have been examined to enhance a structure's ability to withstand earthquake excitations. Comparison of the response due to non-uniform input ground motion with that due to uniform input demonstrates the importance of accounting for spatial variability of excitations. The performance of the optimized designed control systems for uniform input excitations gets worse dramatically over almost all of the evaluation criteria under multiple-support excitations.

Keywords: structural control; cable-stayed bridges; response demands; traveling wave excitation

1. Introduction

Bridges are one of the most seismically vulnerable and important infrastructures in ensuring a functioning society. The increasing awareness in the vulnerability of structures in moderate seismic events was initiated by past earthquake events (Kun *et al.* 2015). Long-span cable-stayed bridges have increased in both number and span lengths. However, they are characterized by longer natural time period and low structural damping which make them highly flexible and susceptible to large amplitude oscillation under seismic loadings (Javanmardi *et al.* 2017). The deck connection between tower and piers greatly affected the seismic performance of the cable-stayed bridges. The rigid connection of deck and tower limited the horizontal deck displacement under earthquake excitation and led to transmission of forces from superstructure to substructure, and hence increased the base shear of the tower (Sharabash and Andrawes 2009, Li *et al.* 2009). On the other hand, the movable or floating configuration had higher deck flexibility and enlarged the horizontal deck displacement under service loadings (Okamoto and Nakamura 2011).

*Corresponding author, Professor, E-mail: shehatarahem@yahoo.com

Researchers have also explored effective seismic control strategies for cable-stayed bridges in order to optimize the mechanical properties and location of the bearings. (Ali and Abdel-Ghaffar 1995, Jung *et al.* 2004, Chang and Loh 2006, Ferreira and Simoes 2011) and experimental tests have been carried out (Heo *et al.* 2014). Semi-active systems are an attractive alternative for structural vibration reduction due to its mechanical simplicity, low power requirements and large control force capacity (Spencer and Nagarajaiah 2003). Past research studies have demonstrated that seismic ground motion can vary significantly over distances comparable to the length of highway bridges on multiple supports. In several cases, these differential asynchronous motions at the bridge supports can induce additional internal forces in the structure compared to the case where all supports are subjected to identical support ground motion. This in turn might have a potentially detrimental effect on the safety of a bridge during a severe earthquake event (Abdel Raheem and Hayashikawa 2007, Abdel Raheem *et al.* 2008&2009, Zhang *et al.* 2009, Wang *et al.* 2009, Li and Chouw 2014). The evaluation of seismic performance becomes particularly important for these types of structures, as the distances between their multiple support points are great, sometimes even greater than the seismic wavelength. Therefore, a uniform excitation evaluation method is not suitable and the traveling wave effect must be considered (Abdel Raheem 2014, Raftoyiannis *et al.* 2014, Wang *et al.* 2015). The main causes of spatial variability are considered: the incoherence effect, which represents random differences in the amplitudes and phases of seismic waves due to reflections and refractions that occur during wave propagation in the heterogeneous medium of the ground and due to differential superposition of waves arriving from different parts of an extended source; the wave-passage effect, which describes the differences in the arrival times of waves at separate locations.

The spatial variation of seismic ground motions been studied by many researchers. Most research is focused on stochastic methods in the frequency domain (Liao and Li 2002, Zhanardo *et al.* 2002, Dumanogluid and Soyluk 2003, Zhang *et al.* 2009). Meanwhile, several response spectrum methods that take into account the effect of correlated ground motion have been developed (Berrah and Kausel 1992, Der Kiureghian 1996). However, both the stochastic methods and response spectrum methods use a linear hypothesis. This assumption is not valid for most structures that are relatively flexible and behave nonlinearly. In such cases, time domain analysis using step-by-step numerical integration techniques is essential. For time domain analyses, correlated earthquake ground motions should be simulated from a variety of positions along the span of a given structure (Shama 2007, Yongxin *et al.* 2011, Abdel Raheem *et al.* 2011). The velocity of the travelling wave plays an important role in the transverse response of the long bridges. When the travelling wave velocity was greater than 1000 m/s the response was dominated by the dynamic component while the response was dominated by pseudo-static component when the travelling wave velocity was less than 300 m/s (Wang *et al.* 2009).

Benchmark structural control problems for cable-stayed bridges have allowed researchers to compare the efficiency of control algorithms and devices (Dyke *et al.* 2003). This study scope is to use ASCE benchmark bridge model (Caicedo *et al.* 2003) to investigate the feasibility and efficiency of different control strategies for seismic protection of cable-stayed bridges under multiple support excitations. The effect of ground motion spatial variation including wave passage and coherence loss on the effectiveness of seismic control systems of cable-stayed bridges is studied to enhance a structure's ability to withstand dynamic loading, the prospects for active; semi-active and passive control systems of the bridge motion are explored. A systematic comparison of the performance of passive and active systems in reducing the structure's responses is performed.

2. Finite element modeling procedures

Based on detailed drawings of the cable-stayed bridge, which is located in Cape Griardeau, Missouri, USA, a 3D finite element model has been developed by Caicedo *et al.* (2003) to represent the complex behavior of the full-scale benchmark bridge shown in Fig. 1. The linear evaluation model was developed as a basis of performance comparison using various protective systems. Three earthquake records, each scaled to peak ground accelerations of 0.36g or smaller, used for numerical simulations are (i) El Centro NS (1940), (ii) Mexico City (1985), and (iii) Gebze N-S (1999). Evaluation criteria J_1 to J_{18} have been established; however, only the evaluation criteria J_1 to J_{13} are relevant to semi-active and passive systems and hence used in the present study, these evaluation criteria have been normalized by the corresponding response quantities for the uncontrolled bridge.

2.1 Equation of motion

The equation of motion for a cable-stayed bridge subjected to uniform seismic excitation can be written as

$$\mathbf{M}\ddot{\mathbf{U}} + \mathbf{C}\dot{\mathbf{U}} + \mathbf{K}\mathbf{U} = -\mathbf{M}\Gamma\ddot{\mathbf{U}}_g + \Lambda\mathbf{f} \quad (1)$$

where \mathbf{U} is the displacement response vector; \mathbf{M} , \mathbf{C} and \mathbf{K} are the mass, damping and stiffness matrices of the structure, \mathbf{f} is the vector of control force inputs, $\ddot{\mathbf{U}}_g$ is the longitudinal ground acceleration, Γ is a vector of zeros and ones relating the ground acceleration to the bridge degrees of freedom (DOF), and Λ is a vector relating the force produced by the control device to the bridge DOFs. For the analysis of the bridge with multiple-support excitation, the model must include the supports degrees of freedom. The seismic movement of the bridge supports excites the superstructure of the bridge through the influence matrix.

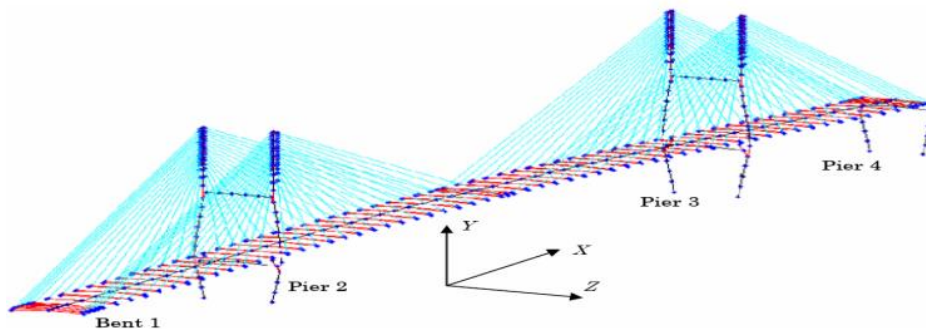


Fig. 1 Bridge finite element model

2.2 Description of the bridge model

The model resulting from the finite element formulation, which is modelled by beam elements, cable elements, and rigid links as shown in Fig. 1, has a large number of degrees-of-freedom and high frequency dynamics. Application of static condensation reduction scheme to the full model of

the bridge resulted in a 419 DOF reduced order model, the first 100 natural frequencies of the reduced model (up to 3.5 Hz) were compared and are in good agreement with those of the 909 DOF structure. The damping in the system is defined based on the assumption of modal damping, the damping matrix was developed by assigning 3% of critical damping to each mode, and this value is selected to be consistent with assumptions made during the bridge design. A reduced-order model, design model of 30 states, of the system was derived from the evaluation model by forming a balanced realization of the system and condensing out the states with relatively small controllability and observability Grammians.

3. Spatial ground motion support excitation

The cross-power spectral density function of spatial ground motions at point i and j on ground surface can be written as

$$S_{ij}(\omega) = S_g(\omega)\gamma_{ij}(\omega, d_{ij}) \quad (2)$$

The coherency-loss function at points i and j was derived from SMART-1 array data as follow

$$\gamma_{ij}(\omega, d_{ij}) = |\gamma_{ij}(\omega, d_{ij})| \cdot \exp\left(-\frac{i\omega d_{ij}}{v}\right) \quad (3)$$

$$|\gamma_{ij}(\omega, d_{ij})| = \exp(-\beta d_{ij}) \cdot \exp\{-\alpha(\omega)\sqrt{d_{ij}}(\omega/2\pi)\}. \quad (4)$$

In which d_{ij} is the projected distance in the wave propagation direction between points i and j on ground surface, β is a constant, and $\alpha(\omega)$ is a function with the following form

$$\alpha(\omega) = \begin{cases} \frac{2\pi a}{\omega} + \frac{b\omega}{2\pi} + c, & 0.314 \frac{\text{rad}}{\text{s}} \leq \omega \leq 62.83 \quad \text{rad/s} \\ 0.1a + 10b + c\omega \geq 62.83 & \text{rad/s} \end{cases} \quad (5)$$

a , b , c , and β can be obtained by least-squares fitting the coherency function of recorded motion. To study the influences of ground motion spatial variation on the seismic performance of structural control of cable-stayed bridges, an intermediate correlated ground motions are considered. Wave propagation speed of $v_s = 1000$ m/s was considered to account for spatial variability, the constant values for intermediate correlated ground motions are given as $a = 11.94 \times 10^{-3}$, $b = -1.811 \times 10^{-5}$, $c = 1.177 \times 10^{-4}$, and $\beta = 3.697 \times 10^{-4}$, which were obtained by processing recorded motions during event 45 at the SMART-1 array. In this study input seismic ground motion time histories are generated using a variation of the spectral representation method. An artificial accelerogram time history at bridge supports are obtained by properly modifying real accelerogram time history with coherence loss function due to incoherence and wave passage effects with separation distance. The generated time histories are compatible with prescribed response spectra and duration of strong ground motion and reflect the ground motion spatial variation effects.

4. Structural control strategy

For a seismically excited structure, assuming that the forces provided by the control devices are

adequate to keep the response of the structure from exiting the linear region, the equations of motion can be written in the following state-space form description as follow

$$\dot{x} = \mathbf{A}x + \mathbf{B}f + \mathbf{E}[\ddot{\mathbf{u}}_g^T \quad \dot{\mathbf{u}}_g^T]^T \tag{6}$$

$$y_m = \mathbf{C}_y x + \mathbf{D}_y f + v \tag{7}$$

$$z = \mathbf{C}_z x + \mathbf{D}_z f \tag{8}$$

In which x is the state vector, y_m is the vector of measured outputs, z is the regulated output vector, v is the measurement noise vector. The measurements typically available for control force determination include the absolute acceleration of selected points on the structure, the displacement of each control device, and a measurement of each control force. A description of the approach used to model and control each of control devices is provided as follow.

4.1 Semi-active control system

The H_2/LQG control algorithm based on the minimization of a performance index is used for the controller design using the reduced order model of the system. The active control force f_c is found by minimizing the performance index subjected to a second order system. A nonlinear control law is derived to maximize the energy dissipated from a vibrating structure by the frictional interface using the normal force as control input. The required normal force is determined using optimal controller; the LQG control problem is to devise a control law with constant gain to minimize the quadratic cost function in the form

$$f_c = -\mathbf{K}x \tag{9}$$

\mathbf{K} is the full state feedback gain matrix for the deterministic regulator problem. An infinite horizon performance index is chosen that weights the regulated output vector, z

$$J = \lim_{\tau \rightarrow \infty} \frac{1}{\tau} \mathbf{E} \left[\int_0^\tau \{(\mathbf{C}_z x + \mathbf{D}_z f)' \mathbf{Q} (\mathbf{C}_z x + \mathbf{D}_z f) + f_c^T \mathbf{R} f_c\} dt \right] \tag{10}$$

where \mathbf{Q} and \mathbf{R} are weighting matrices for the vectors of regulated responses and control forces, respectively. Bouc-Wen's model is used to characterize the hysteretic force-deformation characteristic of the devices. The forces mobilized in the control device (UHYDE-fbr and LRB) can be modelled by biaxial model

$$f_x = c_0 \dot{u}_x + k_0 u_x + \alpha z_x, \quad f_y = c_0 \dot{u}_y + k_0 u_y + \alpha z_y \tag{11}$$

Where z_i is an evolutionary shape variable, internal friction state, bounded by the values ± 1 ; and account for the conditions of separation and reattachment. The model for biaxial interaction of the resultant hysteretic forces is given as 1st differential equation

$$\begin{bmatrix} \dot{z}_x \\ \dot{z}_y \end{bmatrix} = \begin{bmatrix} A \dot{u}_x \\ A \dot{u}_y \end{bmatrix} - \begin{bmatrix} z_x^2 (\gamma \text{sign}(z_x \dot{u}_x) + \beta) & z_x z_y (\gamma \text{sign}(z_y \dot{u}_y) + \beta) \\ z_x z_y (\gamma \text{sign}(z_x \dot{u}_x) + \beta) & z_y^2 (\gamma \text{sign}(z_y \dot{u}_y) + \beta) \end{bmatrix} \begin{Bmatrix} \dot{u}_x \\ \dot{u}_y \end{Bmatrix} \tag{12}$$

c_0, k_0, β, γ and A are called the characteristic parameters of the Bouc-Wen model. β controls the

nature of the constitutive law (hardening or softening). The determination of the most appropriate yielding level or slip load level at different placement locations in the structure is, thus, an important design issue which must be resolved for devices effective utilization in practice. The average friction coefficient is determined to be 0.45; the normal force is proportional to the input voltage. The dynamics involved in the UHYDE-fbr (Dorka *et al.* 1998, Abdel Raheem and Dorka 2006, Abdel Raheem *et al* 2007) pneumatic servo system equilibrium are accounted for through the first order filter. Analog voltage control is applied to air pressure regulator to set the desired analog output air pressure signal, Fig. 2. $\alpha = \mu N$ is a function of N the clamping force and μ the coefficient of sliding friction, c_0 describes the force associated with viscous dissipation due to compressed gas. The UHYDE-fbr device has a capacity of 1000 kN and displacement capacity of 500 mm (the tested friction device scaled: 2.5 for the frictional force; 1.5 for displacement), as follow: $A = 1000 \text{ m}^{-1}$ and $\gamma = \beta = 500 \text{ m}^{-1}$, $c_{0a} = 10 \text{ kN.s/m}$, $c_{0b} = 25 \text{ kN.s/m.volt}$, $k_0 = 25 \text{ kN/m}$, $\alpha_a = 22.5 \text{ kN}$, $\alpha_b = 101.25 \text{ kN/volt}$.

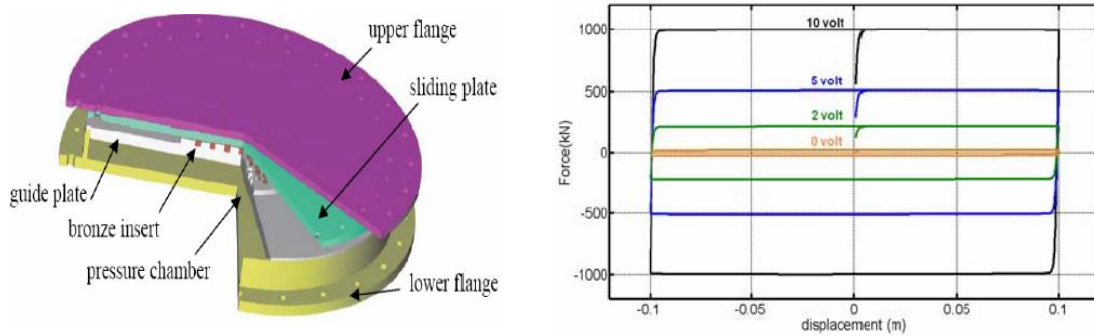


Fig. 2 Physical and idealized hysteresis models UHYDE-fbr friction device

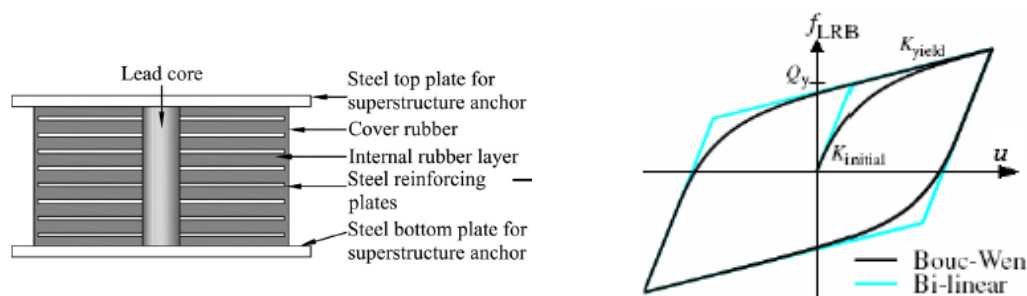


Fig. 3 Physical and idealized hysteresis models of lead rubber bearing (LRB)

4.2 Passive control system

Seismic isolation is an approach which reduces the seismic force to or near the elastic capacity of the structure member, thereby eliminating inelastic deformation. The main aim of utilizing the isolation system is to decrease the fundamental frequency of structural vibration to a value lower than predominate energy-containing frequency of earthquake. Lead Rubber Bearings (LRBs) are considered to passively reduce seismic responses of the studied bridge, Fig. 3. The design

procedure of LRB devices are based on the Guide Specifications Seismic Isolation Design (GSID) AASHTO (2010) and LRFD Bridge Design Specifications (LRFD) AASHTO (2012). The design shear force level for the yielding of lead plugs is taken 10% of the deck weight carried by bearings. The horizontal restoring force is expressed as the sum of three forces acting in parallel in which, k_0 and c_0 are the horizontal stiffness and viscous damping coefficient of the rubber composite of the bearing. $\alpha = (1 - k_0/k_e)$. Q_y is the yield force of the lead plug; Q_y is the yield force from both the lead plug and the rubber stiffness. The properties of the LRB are k_e initial elastic shear stiffness and k_0 post-yield shear stiffness, $k_0/k_e = 0.10$. To model the initial stiffness properly, it is required that $A = k_e/Q_y$, $A = 140 \text{ m}^{-1}$ and $\gamma = \beta = 70 \text{ m}^{-1}$, $c_0 = 100 \text{ kN.s/m}$, $k_e = 68 \text{ MN/m}$, and $Q_y = 400 \text{ kN}$.

5. Numerical analysis for the seismic responses

To verify the effectiveness of the presented seismic control design, simulations are done for the three earthquakes specified in the benchmark problem statement. An intermediate correlated ground motions are considered. The apparent wave velocity is $v = 1000 \text{ m/s}$, the input seismic ground motion time histories are generated using a variation of the spectral representation method. An artificial accelerogram time history at bridge supports are obtained by properly modifying real accelerogram time history with coherence loss function due to incoherence and wave passage effects with separation distance. To evaluate the ability of various control systems to reduce the peak responses, the normalised responses over the entire time record, and the control requirements, thirteen evaluation criteria $J_1 - J_{13}$ are considered in this study, the first six evaluation criteria consider the ability of the controller to reduce peak responses: Evaluation criteria $J_1 - J_6$ are related to peak response quantities, where J_1 = the peak base shear of towers, J_2 = the peak shear force of towers at the deck level, J_3 = the peak overturning moment at the bases of towers, J_4 = the peak moment of towers at the deck level, J_5 = the peak deviation in cable tension, and J_6 = the peak displacement of the deck at the abutment.

$$J_1 = \max_{\substack{\text{ElCentro} \\ \text{Mexico} \\ \text{Gebze}}} \left\{ \frac{\max_{i,t} |F_{bi}(t)|}{F_{0b}^{\max}} \right\}, \quad J_2 = \max_{\substack{\text{ElCentro} \\ \text{Mexico} \\ \text{Gebze}}} \left\{ \frac{\max_{i,t} |F_{di}(t)|}{F_{0d}^{\max}} \right\}, \quad J_3 = \max_{\substack{\text{ElCentro} \\ \text{Mexico} \\ \text{Gebze}}} \left\{ \frac{\max_{i,t} |M_{bi}(t)|}{M_{0b}^{\max}} \right\}, \quad J_4 = \max_{\substack{\text{ElCentro} \\ \text{Mexico} \\ \text{Gebze}}} \left\{ \frac{\max_{i,t} |M_{di}(t)|}{M_{0d}^{\max}} \right\}$$

$$J_5 = \max_{\substack{\text{ElCentro} \\ \text{Mexico} \\ \text{Gebze}}} \left\{ \max_{i,t} \left| \frac{T_{ai} - T_{0i}}{T_{0i}} \right| \right\}, \quad J_6 = \max_{\substack{\text{ElCentro} \\ \text{Mexico} \\ \text{Gebze}}} \left\{ \max_{i,t} \left| \frac{x_{bi}(t)}{x_{0i}} \right| \right\}$$

where $F_{bi}(t)$ and $F_{di}(t)$, $M_{bi}(t)$ and $M_{di}(t)$ are the base shear and moment, shear and moment at the deck level in the i -th tower, F_{0b}^{\max} and M_{0b}^{\max} , F_{0d}^{\max} and M_{0d}^{\max} are the maximum uncontrolled base shear and moment, shear and moment at the deck level in the two towers. T_{0i} is the nominal pretension in the i -th cable, $T_{ai}(t)$ is the actual tension in the cable, and x_{0i} is the maximum of the uncontrolled deck response at these locations. Evaluation criteria $J_7 - J_{11}$ are related to normed response quantities corresponding to response quantities for $J_1 - J_5$.

$$J_7 = \max_{\substack{\text{ElCentro} \\ \text{Mexico} \\ \text{Gebze}}} \left\{ \frac{\max_i \|F_{bi}(t)\|}{\|F_{0b}\|} \right\}, \quad J_8 = \max_{\substack{\text{ElCentro} \\ \text{Mexico} \\ \text{Gebze}}} \left\{ \frac{\max_i \|F_{di}(t)\|}{\|F_{0d}\|} \right\}, \quad J_9 = \max_{\substack{\text{ElCentro} \\ \text{Mexico} \\ \text{Gebze}}} \left\{ \frac{\max_i \|M_{bi}(t)\|}{\|M_{0b}\|} \right\}, \quad J_{10} = \max_{\substack{\text{ElCentro} \\ \text{Mexico} \\ \text{Gebze}}} \left\{ \frac{\max_i \|M_{di}(t)\|}{\|M_{0d}\|} \right\}$$

$$J_{11} = \max_{\substack{\text{ElCentro} \\ \text{Mexico} \\ \text{Gebze}}} \left\{ \max_i \left\{ \frac{\|T_{oi} - T_{oi}\|}{T_{oi}} \right\} \right\}, \quad \|\cdot\| \equiv \sqrt{\frac{1}{t_f} \int_0^{t_f} (\cdot)^2 dt}$$

Evaluation criteria $J_{12} - J_{13}$ are related to control system requirements; J_{12} = the peak control force, J_{13} = the peak device stroke.

$$J_{12} = \max_{\substack{\text{ElCentro} \\ \text{Mexico} \\ \text{Gebze}}} \left\{ \max_{i,t} \left(\frac{f_i(t)}{W} \right) \right\}, \quad J_{13} = \max_{\substack{\text{ElCentro} \\ \text{Mexico} \\ \text{Gebze}}} \left\{ \max_{i,t} \left(\frac{|y_i^d(t)|}{x_0^{\max}} \right) \right\}$$

where $f_i(t)$ is the force generated by the i -th control device over the time history, $W = 510000$ kN is the seismic weight of a bridge based on the mass of the superstructure, $y_i^d(t)$ is the stroke of the i -th control device, x_0^{\max} is the maximum uncontrolled displacement at the top of the towers relative to the ground.

- Passive Control Strategy, 24 LRBs are placed between the deck and pier/bent at eight locations in the bridge, eight between the deck and pier 2, eight between the deck and pier 3, four between the deck and bent 1, and four between the deck and pier 4. The device parameters are optimized for maximum energy dissipation and to minimize the earthquake forces and displacements.

- Active Control Strategy, 24 friction devices are used for semi-active control through the bridge with configuration as in passive strategy, while 24 actuators are for sample active control described in the benchmark. In addition to fourteen accelerometers, eight displacement transducers and eight force transducers to measure control forces applied to the structure are used for feedback to the clipped optimal control algorithm. To evaluate the ability of the friction device system to achieve the performance of a comparable fully active control system, the device is assumed to be ideal, can generate the desired dissipative forces with no delay, hence the actuator/sensor dynamics are not considered. Appropriate selection of parameters (z , Q , R) is important in the design of the control algorithm to achieve high performance controllers. The weighting coefficients of performance index are selected such that; R is selected as an identity matrix; z is comprised of different important responses for the overall behaviour of the bridge that are constructed by the Kalman filter from selected measurements. Extensive simulations have been conducted to find the most effective weighting values corresponding to regulated responses, and accordingly the optimized weighting matrix Q can be selected as follows:

Semi-active control with feedback corresponding to deck displacement and tower top velocity regulated output response and weighting values as follow

$$Q_{dd\&dv} = \begin{bmatrix} q_{dd} \mathbf{I}_{4 \times 4} & \mathbf{0} \\ \mathbf{0} & q_{dv} \end{bmatrix} \quad q_{dd} = 8092.5, \quad q_{dv} = 4.607E5 \quad (13)$$

Sample active control with feedback corresponding to deck displacement and mid span acceleration regulated output response and weighting values as follow

$$Q_{dd\&da} = \begin{bmatrix} q_{dd} \mathbf{I}_{4 \times 4} & \mathbf{0} \\ \mathbf{0} & q_{da} \end{bmatrix} \quad q_{dd} = 3222, \quad q_{da} = 40.00 \quad (14)$$

Simulation results of the proposed control strategies are compared for uniform and multiple

Table 1 Maximum evaluation criteria for El cento / Mexico / Gebze earthquakes

Criteria		Passive Control	Semi-Active Control	Sample Active Control
J ₁	Uniform	0.28 / 0.46 / 0.42	0.29 / 0.42 / 0.50	0.27 / 0.36 / 0.42
	Multiple excitation $v_s=1000$ m/s	0.33 / 0.36 / 0.46	0.33 / 0.50 / 0.54	0.32 / 0.37 / 0.49
J ₂	Uniform	0.83 / 1.29 / 1.06	0.91 / 1.20 / 1.12	0.76 / 0.88 / 0.74
	Multiple excitation $v_s=1000$ m/s	1.20 / 1.03 / 1.04	0.84 / 1.21 / 1.03	1.11 / 1.03 / 0.96
J ₃	Uniform	0.31 / 0.62 / 0.47	0.23 / 0.42 / 0.36	0.28 / 0.42 / 0.39
	Multiple excitation $v_s=1000$ m/s	0.38 / 0.40 / 0.44	0.27 / 0.35 / 0.37	0.34 / 0.37 / 0.45
J ₄	Uniform	0.70 / 0.80 / 0.76	0.48 / 0.63 / 0.65	0.57 / 0.74 / 0.79
	Multiple excitation $v_s=1000$ m/s	0.57 / 0.57 / 0.79	0.47 / 0.59 / 0.80	0.57 / 0.67 / 0.86
J ₅	Uniform	0.28 / 0.11 / 0.21	0.27 / 0.14 / 0.22	0.23 / 0.10 / 0.19
	Multiple excitation $v_s=1000$ m/s	0.33 / 0.18 / 0.22	0.30 / 0.17 / 0.22	0.31 / 0.18 / 0.22
J ₆	Uniform	1.65 / 2.51 / 1.85	1.10 / 1.00 / 1.71	1.17 / 1.79 / 2.29
	Multiple excitation $v_s=1000$ m/s	1.36 / 1.45 / 1.69	0.62 / 0.98 / 1.40	1.02 / 1.49 / 2.23
J ₇	Uniform	0.26 / 0.41 / 0.41	0.23 / 0.35 / 0.33	0.21 / 0.25 / 0.30
	Multiple excitation $v_s=1000$ m/s	0.29 / 0.39 / 0.40	0.24 / 0.31 / 0.32	0.26 / 0.30 / 0.33
J ₈	Uniform	0.84 / 1.00 / 1.05	0.85 / 1.03 / 0.96	0.79 / 0.83 / 0.86
	Multiple excitation $v_s=1000$ m/s	0.95 / 1.02 / 1.08	0.95 / 1.16 / 1.08	1.01 / 1.03 / 1.01
J ₉	Uniform	0.28 / 0.50 / 0.47	0.20 / 0.30 / 0.34	0.23 / 0.30 / 0.39
	Multiple excitation $v_s=1000$ m/s	0.30 / 0.43 / 0.47	0.21 / 0.26 / 0.35	0.27 / 0.33 / 0.42
J ₁₀	Uniform	0.51 / 0.76 / 0.54	0.51 / 0.56 / 0.68	0.60 / 0.75 / 0.70
	Multiple excitation $v_s=1000$ m/s	0.48 / 0.52 / 0.70	0.49 / 0.58 / 0.71	0.60 / 0.75 / 0.87
J ₁₁ (10 ⁻²)	Uniform	2.56 / 1.65 / 1.88	2.68 / 1.52 / 1.76	2.64 / 1.38 / 1.68
	Multiple excitation $v_s=1000$ m/s	3.13 / 2.18 / 2.16	2.82 / 1.62 / 2.06	3.16 / 1.76 / 2.07
J ₁₂ (10 ⁻³)	Uniform	2.92 / 2.45 / 2.42	1.96 / 1.96 / 1.96	2.84 / 1.64 / 2.88
	Multiple excitation $v_s=1000$ m/s	2.53 / 1.72 / 2.27	1.96 / 1.96 / 1.96	1.80 / 1.43 / 2.06
J ₁₃	Uniform	1.01 / 1.37 / 0.81	0.67 / 0.55 / 0.75	0.72 / 0.97 / 0.99
	Multiple excitation $v_s=1000$ m/s	0.83 / 0.79 / 0.74	0.38 / 0.53 / 0.61	0.62 / 0.81 / 0.97

excitations. Table 1 shows the evaluation criteria for all the three earthquakes, from which, it can be concluded that the different control strategies are very effective in reducing the force and displacement response, especially for ground motions with a high frequency content such as El Centro with dominant frequencies of 1.1, 1.3 and 2.1 Hz, as shown in Table 1, while the efficiency of control strategies under Mexico earthquake (dominant frequency of 0.45 Hz) and Gebze earthquake (dominant frequencies of 0.25 and 2.0 Hz) that has a lower frequency content, is decreased and resulting in a larger force and displacement responses dominated by low-order modes compared to El Centro earthquake case as shown in Table 1. It is also shown the dependency of the seismic response of the controlled bridge on the frequency content of the input motion, since lower and higher order fundamental modes with frequencies close to Gebze earthquake wide range dominant frequencies are excited, resulting in higher force and displacement responses, and higher control force is required. The maximum deck displacement is

less than allowable displacement (0.3 m), the tension in the stay cables remains within allowable values.

A comparative study is also performed on Cable-stayed bridge benchmark equipped with passive, semi-active or active control system with the control device numbers and configurations. The passive control strategy can be designed to achieve peak response (J_1 – J_6) reduction comparable to the active/semi-active control strategy, while it is difficult to attain the same response reduction efficiency over the entire time history (J_7 – J_{11}), the member force responses can be minimized, but of course in the expense of increasing deck displacement. The passive control system creates a larger deck displacement reduction response compared to active controlled system, while sacrificing the acceleration and force responses of the bridge structure. To reduce the excessive displacement, higher stiffness is needed between the deck and the towers. An optimum performance with passive control system can be obtained by balancing the reduction in forces along the bridge against tolerable displacements. For the cable-stayed bridge control, it is observed that unlike the passive damper case, the proposed active/semi-active control strategies are able to effectively and simultaneously reduce the maximum displacement and force responses. But the passive control system for this benchmark problem is a little better than the semi-active control strategy in some responses. It is observed that passive control strategy is quite effective in reducing response quantities of the bridge whenever predominant period of ground motions is close to the fundamental natural period of the bridge. The analyses performed shows that the spatial variation of the earthquake ground motion can significantly affects the structural response; consequently, efficient control systems must be appropriately designed and tuned. From the statistical analysis of the variation of the evaluation criteria of different control strategies, the semi-active control has almost the same robustness stability of active control regard of the spatial variability of earthquake ground motions.

The results show that responses considering the travelling wave effect significantly differ from those under uniform excitation. The spatial variation of ground motion affects the internal force demands, and consequently could affect the control efficiency. However, the evaluation criteria of seismic responses of the bridge do not always follow the same changing rules with the decrease of the surface apparent wave velocity. The responses may be amplified under the excitation of ground motion but may be reduced under another excitation. Nevertheless, in most engineering cases this effect is still ignored by the practical structural designers since seismic design codes remain unsatisfactory in terms of the ground motion spatial variations. This ignorance could reduce the degree of seismic safety and control system reliability of CSB structure.

6. Conclusions

The overall seismic performance of the cable-stayed bridge is remarkably improved by utilizing the control systems that perform well when earthquake motions are uniform at all supports along the entire cable-stayed bridge. But, bridges subjected to spatially variable input motions are characterized by excitation of higher modes which are primarily anti-symmetric. The analyses performed shows that the spatial variation of the earthquake ground motion can significantly affects the structural response; consequently, efficient control systems must be appropriately designed and tuned. The performance of the control systems that designed for uniform excitations gets worse dramatically over almost all of the evaluation criteria under multiple-support excitations. From the statistical analysis of the variation of the evaluation criteria of different

control strategies, the semi-active control has almost the same robustness stability of active control regard of the spatial variability of earthquake ground motions. The assumption of uniform earthquake motion along the entire bridge, however, may be unrealistic for long span bridges since the differences in ground motion among different supports due to travelling seismic waves may result in quantitative and qualitative differences in seismic response as compared with those produced by uniform motion at all supports. Design codes and retrofiting techniques must be upgraded to take into account the spatial character of the seismic input.

References

- AASHTO (2010), *Guide Specifications for Seismic Isolation Design*, 3rd Edition, American Association of State Highway and Transportation Officials, Washington, U.S.A.
- AASHTO (2012), *LRFD Bridge Design Specifications*, American Association of State Highway and Transportation Officials, Washington, U.S.A.
- Abdel Raheem, S.E., Hayashikawa, T. and Dorka, U. (2008), "Spatial variation effects on seismic response control of cable-stayed bridges", *Proceedings of the 14th World Conference on Earthquake Engineering*, Beijing, China, October.
- Abdel Raheem, S.E. (2014), "Ground motion spatial variation effects on seismic performance of structural control of cable-stayed bridges", *Proceedings of the 9th International Conference on Structural Dynamics*, Porto, Portugal, June-July.
- Abdel Raheem, S.E. and Dorka, U.E. (2006), "Feasibility study on semi-active control of the cable-stayed bridge benchmark with friction device system", *Proceedings of the 4th World Conference on Structural Control and Monitoring*, San Diego, California, U.S.A., July.
- Abdel Raheem, S.E. and Hayashikawa, T. (2007), "Seismic protection of cable-stayed bridges under multiple-support excitations", *Proceedings of the 4th International Earthquake geotechnical Engineering*, Thessaloniki, Greece, June.
- Abdel Raheem, S.E., Dorka, U.E. and Hayashikawa, T. (2007), "Friction based semi-active control of cable-stayed bridges", *JCSE J. Struct. Eng.*, **53A**, 428-438.
- Abdel Raheem, S.E., Hayashikawa, T. and Dorka, U.E. (2009), "Earthquake ground motion spatial variation effects on seismic response control of cable-stayed bridges", *JCSE J. Struct. Eng.*, **55A**, 709-718.
- Abdel Raheem, S.E., Hayashikawa, T. and Dorka, U.E. (2011), "Ground motion spatial variability effects on seismic response control of cable-stayed bridges", *Earthq. Eng. Eng. Vibr.*, **10**(1), 37-49.
- Ali, H.M. and Abdel-Ghaffar, A.M. (1995), "Seismic passive control of cable-stayed bridges", *Shock Vibr.*, **2**(4), 259-272.
- Berrah, M. and Kausel, E. (1992), "Response spectrum analysis of structures subjected to spatially varying motions", *Earthq. Eng. Struct. Dyn.*, **21**(6), 461-470.
- Caicedo, J.M., Dyke, S.J., Moon, S.J., Bergman, L.A., Turan, G. and Hague, S. (2003), "Phase II benchmark control problem for seismic response of cable-stayed bridges", *J. Struct. Contr.*, **10**(3-4), 137-168.
- Chang, C.M. and Loh, C.H. (2006), "Seismic response control of cable-stayed bridge using different control strategies", *J. Earthq. Eng.*, **10**(4), 481-508.
- Der Kiureghian, A. (1996), "A coherency model for spatially varying ground motions", *Earthq. Eng. Struct. Dyn.*, **25**(1), 99-111.
- Dorka, U.E., Flygare, E. and Ji, A. (1998), "Passive seismic control of bridges by hysteretic device system", *Proceedings of the 2nd World Conference on Structural Control*, Kyoto, Japan, June-July.
- Dumanoglu, A.A. and Soyuluk, K. (2003), "A stochastic analysis of long span structures subjected to spatially varying ground motions including the site-response effect", *Eng. Struct.*, **25**(10), 1301-1310.
- Dyke, S.J., Caicedo, J.M., Turan, G., Bergman, L.A. and Hague, S. (2003), "Phase I benchmark control problem for seismic response of cable-stayed bridges", *ASCE J. Struct. Eng.*, **129**(7), 857-872.

- Ferreira, F.L.S. and Simoes, L.M.C. (2011), "Optimum design of a controlled cable stayed bridge subject to earthquakes", *Struct. Multidiscipl. Optim.*, **44**(4), 517-528.
- Heo, G., Kim, C. and Lee, C. (2014), "Experimental test of asymmetrical cable-stayed bridges using MR-damper for vibration control", *Soil Dyn. Earthq. Eng.*, **57**, 78-85.
- Javanmardi, A., Ibrahim, Z., Ghaedi, K., Jameel, M., Khatibi, H. and Suhatri, M. (2017), "Seismic response characteristics of a base isolated cable-stayed bridge under moderate and strong ground motions", *Arch. Civil Mech. Eng.*, **17**(2), 419-432.
- Jung, H.J., Park, K.S., Spencer, J.B.F. and Lee, I.W. (2004), "Hybrid seismic protection of cable-stayed bridges", *Earthq. Eng. Struct. Dyn.*, **33**(7), 795-820.
- Kun, C., Li, B. and Chouw, N. (2015), "Seismic fragility analysis of bridge response due to spatially varying ground motions", *Coupled Syst. Mech.*, **4**(4), 297-316.
- Li, B. and Chouw, N. (2014), "Effect of soil flexibility on bridges subjected to spatially varying excitations", *Coupled Syst. Mech.*, **3**(2), 213-232.
- Li, H., Liu, J. and Ou, J. (2009), "Investigation of seismic damage of cable-stayed bridges with different connection configuration", *J. Earthq. Tsunami*, **3**(3), 227-247.
- Liao, S. and Li, J. (2002), "A stochastic approach to site-response component in seismic ground motion coherency model", *Soil Dyn. Earthq. Eng.*, **22**(9-12), 813-820.
- Okamoto, Y. and Nakamura, S. (2011), "Static and seismic studies on steel/concrete hybrid towers for multi-span cable-stayed bridges", *J. Constr. Steel Res.*, **67**(2), 203-210.
- Raftoyiannis, I.G., Konstantakopoulos, T.G. and Michaltsos, G.T. (2014), "Dynamic response of cable-stayed bridges subjected to sudden failure of stays - the 2D problem", *Coupled Syst. Mech.*, **3**(4), 345-365.
- Shama, A.A. (2007), "Simplified procedure for simulating spatially correlated earthquake ground motions", *Eng. Struct.*, **29**(2), 248-258.
- Sharabash, A.M. and Andrawes, B.O. (2009), "Application of shape memory alloy dampers in the seismic control of cable-stayed bridges", *Eng. Struct.*, **31**(2), 607-616.
- Spencer, J.B.F. and Nagarajaiah, S. (2003), "State of art of structural control", *ASCE J. Struct. Eng.*, **129**(7), 845-856.
- Sun, H., Wang, D.J. and Li, Y. (2013), "Seismic performance analysis of a multi-span continuous girder bridge under multi-excitation", *Key Eng. Mater.*, **540**, 141-152.
- Wang, H., Li, J., Tao, T., Wang, C. and Li, A. (2015), "Influence of apparent wave velocity on seismic performance of a super-long-span triple-tower suspension bridge", *Adv. Mech. Eng.*, **7**(6), 1-14.
- Wang, J., Can, A.J., Cooke, N. and Moss, P.J. (2009), "The response of a 344 m long bridge to non-uniform earthquake ground motions", *Eng. Struct.*, **31**(11), 2554-2567.
- Yongxin, W., Yufeng, G. and Dayong, L. (2011), "Simulation of spatially correlated earthquake ground motions for engineering purposes", *Earthq. Eng. Eng. Vibr.*, **10**(2), 163-173.
- Zanardo, G., Hao, H. and Modena, C. (2002), "Seismic response of multi-span simply supported bridges to spatially varying earthquake ground motion", *Earthq. Eng. Struct. Dyn.*, **31**(6), 1325-1345.
- Zhang, Y.H., Li, Q.S., Lin, J.H. and Williams, F.W. (2009), "Random vibration analysis of long-span structures subjected to spatially varying ground motions", *Soil Dyn. Earthq. Eng.*, **29**(4), 620-629.